Investigation of energy transfer from PALS iodine laser beam to shock wave generated in solid target relevant to shock ignition

T. Pisarczyk[1], Z. Kalinowska[1], J. Badziak[1], A. Kasperczuk[1], S. Borodziuk[1], M. Rosiński[1], P. Parys[1], T. Chodukowski[1], S. Yu. Gus'kov[2], N.N. Demchenko[2], D. Batani[3], L. Antonelli[3], P. Koester[4], L. A. Gizzi[4], L. Labate[4], G. Cristoforetti[4], F. Baffigi[4], J.Ullschmied[5], E. Krousky[6] M. Pfeifer[6], O. Renner[6], M. Smid[6], J. Skala[6], and P. Pisarczyk[7]

[1]*Institute of Plasma Physics and Laser Microfusion, Warsaw, Poland*
[2]*P.N. Lebedev Physical Institute of RAS, 53 Leninsky Ave., 119 991 Moscow, Russia*
[3]*CELIA, University Bordeaux-I, Bordeaux, France*
[4]*Intense Laser Irradiation Laboratory at INO-CNR, Pisa, Italy*
[5]*Institute of Physics ASCR, v.v.i., Na Slovance 2, 182 21 Prague 8, Czech Republic*
[6]*Institute of Plasma Physics ASCR, v.v.i., Za Slovankou 3, 182 00 Prague 8, Czech Republic*
[7]*Warsaw University of Technology, ICS, 15/19 Nowowiejska St., 00-665 Warsaw, Poland*

Abstract

The efficiency of the laser energy conversion to a shock wave has been investigated in solid targets irradiated by a single or two consecutive laser beams. The first laser pulse was used to produce the plasma simulating conditions relevant to shock ignition approach. One- and two-layer planar targets (bulk Al and Cu alternatively covered by a thin CH layer) were used. The laser provided a 250 ps pulse within the intensity range of 1-50 PW/cm^2 at the first and third harmonics with wavelengths of 1.315 and 0.438 μm, respectively. Three-frame interferometry and measurements of crater parameters were used as the main diagnostics. The contribution of fast electrons to ablation and the laser energy conversion into shock wave have been investigated for different conditions of the target irradiation, including the pre-plasma presence. 2D numerical simulations and theoretical analysis were carried out to support explanation of experimental results.

1. Introduction

One of the main research aims related to the shock ignition concept (SI) [1,2] is to investigate the mechanism of ablation pressure production by the laser spike of 1-50 PW/cm^2 intensity and of several-hundred-ps duration when a main part of the absorbed laser energy is converted in fast electrons under the presence of the pre-plasma. Energy transfer by fast electrons into the plasma with supercritical density can provide an ablation pressure of several hundreds of Mbar which is necessary for igniting shock generation [3,4]. The recent experiments with OMEGA laser [5,6] have demonstrated an increasing efficiency of the energy transfer to both planar and spherical targets resulting from a contribution of fast electrons generated due to stimulated Raman scattering and two-plasmon decay in an extended pre-plasma.

This work extends our previous research [7, 8] on the role of fast electrons in the laser energy conversion to shock waves performed with PALS iodine laser at intensities of 1-50 PW/cm^2 using the first (1ω) and third (3ω) harmonics radiation. In those experiments massive targets of Al and Cu have been irradiated at various focal spot radii of the laser beam R_L to identify the mechanisms of the laser radiation absorption and to determine their influence on absorbed energy transfer to the target. The mass of the ablated plasma as well as the fraction of the laser energy deposited in solid material have been determined by using the 3-frame-interferometer and by measuring–the–volume_ of the crater created on the solid surface. The experiments have shown a strong influence of the wavelength and the intensity of the laser beam on the efficiency of the laser energy transfer to the massive target, independent from the kind of the material. The 2D numerical simulations with calculations of fast electrons

transport, as well as theoretical analysis based on the analytical model [9] fully confirmed the experimental results and allow to conclude that in the case of 1ω and intensities of 10-50 PW/cm^2 and absence of the pre-plasma on the target surface, the dominant ablation mechanism is heating by fast electrons generated by resonant absorption [8]. For the maximum laser energy 580 J and intensity of 50 PW/cm^2, the ablative pressure reaches about 180 Mbar in spite of two-dimensional expansion of target corona**.** However, for 3ω the ablation pressure originates from thermal electron conductivity heating, and its value of about 50 Mbar is several times lower in comparison with 1ω case.

The results of the next step experiments directed at the study of the pre-plasma influence on the ablation and the energy conversion efficiency to the shock wave are presented below.

2. Experimental results and discussion

In the reported investigation, the planar layered targets consisting of massive Cu and a 25-μm-thick layer of the light CH material were applied. Accordingly to SI concept, the targets were irradiated using two laser pulses. The 1ω laser beam with the energy of ~50 J produced a pre-plasma imitating the corona of the pre-compressed ICF target. The spike-driven shock wave was generated by means of the 1ω or 3ω main pulse with energy of ~ 200 J. The influence of the pre-plasma on the parameters of the shock wave was determined from the crater volume measurements and the electron density distributions obtained for different focal spot radius R_L in the range of 40-160 μm. Interferograms were registered 2 ns after the second laser pulse maximum. The delay Δt=1.2 ns between the main and auxiliary laser beams was selected. Figure 1 presents a comparison of the crater volumes V_{cr} and the N_e/V_{cr} ratios obtained for two wavelengths in the cases of absence and presence of the pre-plasma (N_e-total electron number in plasma torch). Ne Without the pre-plasma, Fig. 1a, the dependences of V_{cr} and N_e/V_{cr} on R_L are similar for both

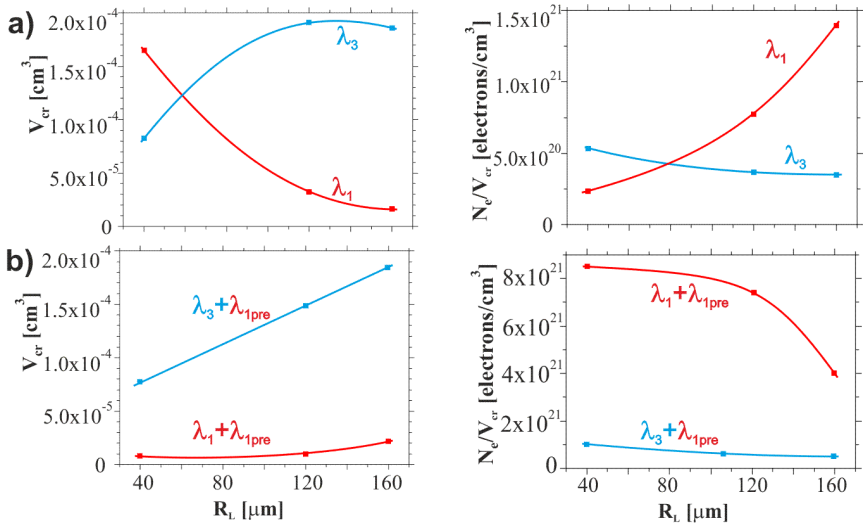

Fig. 1 Dependence of the crater volume and the N_e/V_{cr} ratio on the focal spot radius of the main laser in the case of: a) absence and b) presence of pre-plasma.

Al and Cu targets. For 3ω, i.e., at the predominant inverse bremsstrahlung absorption, the efficiency of the crater creation reduces with the decreasing R_L due to the two-dimensional expansion effect. In contrast, for 1ω the efficiency of the crater creation increases with the decreasing R_L which, according to numerical simulations, directly corresponds to an energy transfer to the target by fast electrons generated due to resonant absorption. The strong influence of the pre-plasma on the crater creation process in the case of 1ω is clearly visible in Fig. 1b. The crater volume decreases by more than one order of magnitude and

simultaneously, N_e/V_{cr} increases by the same rate. It testifies the weakness of the fast electrons role in the energy transport process. In the case of 3ω, the pre-plasma influences the crater formation process only weakly and both V_{cr} and N_e/V_{cr} values remain at the same level as in the case of the pre-plasma absence.

In order to obtain a more detailed information about the ablated plasma state, the quantitative analysis of interferograms has been performed to determine a gradient of the electron density that is the most important characteristics of the plasma state. The maximal axial gradient was derived from the approximation of experimental axial density profiles by the exponential function $y=A_0e^{-z/L}+y_0$ (see Fig. 2a). The parameters of this function determine the maximal electron density gradient in the opacity zone: $[dy/dz]_{z=0}=A_0/L$, where L – scalelength of density gradient and A_0 – maximal electron density. The dependences of the plasma axial density gradient on R_L for the above-mentioned conditions of the target irradiation are shown in Fig. 2. At the pre-plasma absence and 1ω, Fig. 2b, the density gradient increases strongly with the decreasing R_L even for the radii smaller than 80 μm. When compared with 1ω case, at 3ω the plasma expansion is more extended in the direction of z axis in comparison with 1ω and the density gradient increases with the increasing radius of

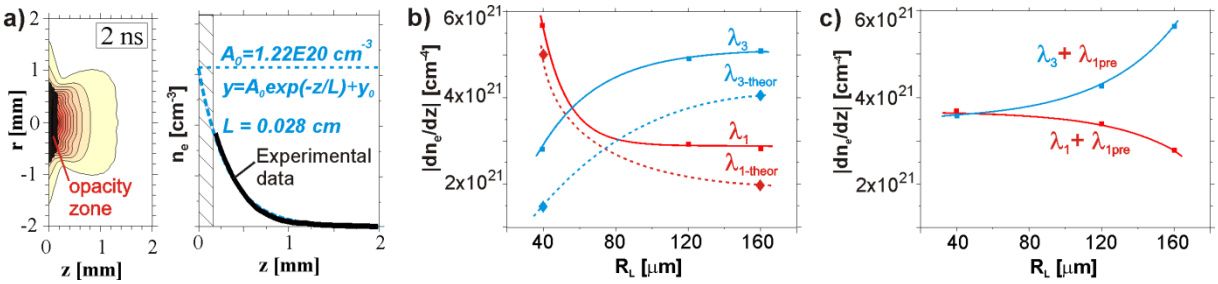

Fig. 2 The maximum density gradient for 1ω and 3ω in the cases of: b) with and c) without pre-plasma.

the focal spot. In the case of the pre-plasma presence, Fig. 2c, the constraint of the plasma radial expansion by the pre-plasma causes an elongation of the plasma stream. In the case of 3ω, the pre-plasma constraint is stronger due to the axial character of expansion. The absorption of the main beam in the long, relatively cold pre-plasma occurs mainly by the inverse bremsstrahlung mechanism for both 1ω and 3ω radiation. Under these conditions the heating is distributed in the area of a significant longitudinal size (Fig. 2c) that leads to the decreasing axial density gradient as compared with the solid target irradiation. Stronger refraction in the case of 1ω - in comparison to 3ω - leads to a stronger re-distribution of the absorbed energy in the lateral direction that is the reason for an additional decrease of the density gradient.

The density gradient was evaluated using a model [9] based on self-similar solutions of isothermal expansion of the given mass material at the planar (corresponding to relatively large focal spot radius of 160 μm) and spherical (R_L=40 μm) geometries. If laser beam irradiates directly a surface of the solid target (the pre-plasma is absent), the density gradient in planar and spherical geometries is given by the following expressions, respectively:

$$\frac{dn_e}{dz} \approx \frac{Z}{Am_p}\frac{m}{\pi R_L^2(2K_aE_Lt/m)} \quad \text{and} \quad \frac{dn_e}{dz} \approx \frac{Z}{Am_p}\frac{m}{\pi(2K_aE_Lt/m)^2}$$

where: Z, A, m_p are the charge, atomic number and proton mass, K_a is the absorption coefficient, t is the current time and m is the mass ablated (evaporated) during the period of the laser pulse duration τ_L. The mass for electron-conductivity-driven ablation (valid for 3ω and 1ω at R_L=160 μm) or fast-electron-driven ablation (valid for 1ω at small radii of 40 and 80 μm) follows from formulae:

$$m_c = 1.1 \times 10^2 \left(\frac{A}{Z+1}\right)^{7/6} \frac{(K_a I_L \tau_L)^{2/3} R_L^2}{(Z+3.3)^{1/3}}, g \quad \text{and} \quad m_e = \pi R_L^2 \mu_e \approx 10^{-5} \frac{A}{Z} R_L^2 (I_L \lambda^2)^{4/3}, g$$

where the expressions $\mu_{e(g/cm)^2} = 5.2 \cdot 10^{-7} \frac{A}{Z} E_{0(keV)}^2$ and $E_{0(keV)} = 8\left(I_{L(pw)} \lambda_{(\mu)}^2\right)^{2/3}$ were used for the fast electron range and average energy. The values I_L, τ_L, R_L and λ are introduced in units of PW/cm^2, ns, cm and μm, respectively. First of all, in the case of small radii the expression for spherical expansion shows that the decreasing radii lead to the strongly increasing density gradients, as R_L^{-2}, at the fast-electron-driven ablation under 1ω-beam irradiation and, in contrast, to the strongly decreasing gradients, as R_L^2, at the electron-conductivity-driven ablation under 3ω irradiation. Consequently at small radii of the laser beam, the density gradient is larger for 1ω-irradiation as compared to 3ω case and at large radii, the relation between the values of gradients is inversed. According to numerical simulations, the absorption coefficients of 1ω and 3ω radiation are about of 0.21 and 0.63 for the beams with the radius of 40 μm and 0.31 and 0.82 for the beams with the radius of 160 μm, respectively. When taking into account this data, the above presented expressions give the values of density gradients equal to 5×10^{21} and 1.5×10^{21} cm^{-4} for 1ω and 3ω radiation at R_L=40μm, and 4×10^{21} and 2×10^{21} cm^{-4} for 3ω and 1ω radiation at R_L=160μm, respectively.

A presence of the pre-plasma creates poor conditions for resonant absorption and, therefore, for the laser energy conversion to fast electrons. This results in suppression of the fast electrons contribution to the ablation process. The significantly smaller effectiveness of the energy transfer to dense plasma regions under the pre-plasma created by the high-intensity 1ω pulse is clearly seen from both the craters volumes and density gradient data.

Conclusions

Two-beam experiments directed to imitate the spike-laser interaction with the pre-produced plasma have shown a significantly decreasing efficiency of the laser energy transport to the solid part of the target for the 1ω main (spike) beam. Similar phenomenon observed in previous experiments using the 1ω single beam was associated with the fast electrons energy transfer to a dense plasma region. Those experiments however have not provided data indicating alteration of the fast electrons generation due to resonant absorption in the relatively short pre-plasma by any other mechanism connected with parametric plasma instabilities.

This work was supported in part by the Access to Research Infrastructure activity in the 7th Framework Program of the EU Contract No. 284464, Laserlab Europe III, by National Centre for Science (NCN), Poland under Grant No 2012/04/M/ST2/00452. The participation of S.Yu. Gus'kov and N.N. Demchenko in this work was supported by RFBR projects No 12-02-92101-JF and No 13-02-00295.

References:

1. V. A. Scherbakov, Sov. J. Plasma Physics **9**, 240 (1983)
2. R. Betti, C.D. Zhou, K.S. Anderson et al, Phys. Rev. Lett. **98**, 155001 (2007)
3. S. Yu. Gus'kov, V. V. Zverev and V. B. Rozanov, Quantum Electronics **13**, 498 (1983)
4. S. Gus'kov, X. Ribeyre, M. Touati et al, Phys.Rev. Lett. **102**, 255004 (2012)
5. W. Theobald, R. Betti, C. Stoeckl et all, Phys. Plasmas **15,** 056306 (2008
6. W. Theobald, R. Nora, M. Lafon et all, Phys. Plasmas **19,** 102706 (2012)
7. Z. Kalinowska, A. Kasperczuk, T. Pisarczyk, T. Chodukowski, S. Yu. Gus'Kov, N. N. Demchenko et al, Nukleonika **57,** 227 (2012).
8. S. Yu. Gus'kov, N. N. Demchenko, A. Kasperczuk, T. Pisarczyk, T. Chodukowski, Z. Kalinowska et al, Laser and Particle Beams (submitted).
9. S. Yu. Gus'kov et al, Quantum Electronic, **34** (11), 989 (2004).